

UC Irvine

UC Irvine Previously Published Works

Title

Flight Procedural Noise Assessment of Blended-Wing—Body Aircraft with Variable Thrust

Permalink

<https://escholarship.org/uc/item/1r70j6pp>

Authors

Pellerito, Victoria

Mott, Mallory

Acosta, Naomi

et al.

Publication Date

2025-02-06

DOI


10.2514/1.C037984

Copyright Information

This work is made available under the terms of a Creative Commons Attribution License, available at <https://creativecommons.org/licenses/by/4.0/>

Peer reviewed

Flight Procedural Noise Assessment of Blended-Wing-Body Aircraft with Variable Thrust

Victoria Pellerito,^{*} Mallory Mott,[†] Naomi Acosta,[‡] and Jacqueline Huynh[§] 

University of California, Irvine, Irvine, California 92617

and

Jack Ahrens,[¶] Franco Staub,^{**} Judy Gallman,^{††} and John Vassberg^{‡‡}

JetZero, Long Beach, California 90808

<https://doi.org/10.2514/1.C037984>

Today's commercial aviation industry centers on the tube-and-wing aircraft configuration with underwing-mounted engines, possibly nearing convergence on optimal performance capabilities with acceptable community noise. A potentially feasible breakthrough for obtaining lower noise levels for commercial aviation is the blended-wing-body (BWB), which presents unique noise-reducing characteristics such as engine shielding and simplified high-lift devices. The significance of characteristics unique to BWBs on overall aircraft noise is assessed through a study of a BWB aircraft design representative of the JetZero vehicle. This paper presents a methodology capable of modeling the aircraft's propulsion system and corresponding performance capabilities necessary to assess the vehicle noise sources and overall community noise impact. Analysis of Part 36 certification noise levels indicates that the vehicle's margin to Stage 5 standards is 35.8 effective perceived noise level (in EPNdB), and an additional 2.0 EPNdB is achievable with a decreased maximum takeoff thrust engine variant. Community noise impacts of departure and arrival procedures are studied through comparison of single-event noise contours. Significant contour area reductions were observed when compared to conventional tube-and-wing aircraft of similar weight and range class. Further departure and approach noise reductions were modeled through additional full-flight procedure variations.

Nomenclature

$L_{A,Max}$	=	maximum A-weighted sound pressure level
V_2	=	takeoff safety speed
V_{REF}	=	reference speed

I. Introduction

THE steady growth and advancements of the aviation industry have continued along with increasing concerns regarding aircraft noise pollution and its impacts on communities surrounding airports [1]. Potential solutions to reducing aircraft-related community noise include the design of advanced aircraft with low-noise features, as well as the implementation of operational procedures for noise abatement [1]. The blended-wing-body (BWB) is an example of an advanced aircraft design with low-noise features. The design differs from the traditional tube-and-wing configuration; the vehicle has overwing-mounted engines that introduce shielding of engine noise, as well as simplified

high-lift devices that reduce airframe noise. These factors allow for potential noise reductions compared to traditional tube-and-wing aircraft, which is conveyed in prior studies conducted by the German Aerospace Center [2,3]. The concept of the BWB configuration has been extensively studied by Boeing, NASA, Airbus, and more recently JetZero, but has not yet found its way to the commercial sector [4–6]. BWB aircraft concepts date back to the 1940s, which laid the foundation for more advanced designs and iterations of BWB configurations. BWB demonstrator vehicles constructed on these concepts include the XP-67 in the 1940s, the BWB-17 in the 1990s, and the X-48 in the 2000s [7,8]. An example of a modern BWB aircraft is the Airbus MAVERIC UAV prototype, which flew in 2019, demonstrating the feasibility of a contemporary BWB aircraft [9,10]. Moreover, NASA Langley has analyzed the noise reduction and fuel efficiency of unconventional aircraft designs through studies on the hybrid wing-body aircraft concept and noise-reducing trajectories such as reduced approach speed [11]. In addition, the Cambridge-MIT Institute Silent Aircraft Initiative developed an optimized aircraft design approach based on noise abatement, which demonstrated the high-lift and noise shielding benefits of BWB configurations [12,13]. Different studies have consistently shown additional benefits of BWB configurations beyond low noise emissions, such as improved fuel efficiency and payload capacity [12,14,15].

Alongside the low-noise features, for a given aircraft design, community noise levels around airports can be further reduced through low-noise approach and departure procedures [16–18]. These community noise reductions can be achieved with adjustments of the flight path via translation of the lateral and vertical track. Such flight procedure modifications are highly coupled with the aircraft's performance, which is significantly influenced by the maximum engine thrust [19].

The focus of this paper is to develop a methodology to assess the noise impact of individual components of the BWB aircraft through the design of propulsor systems and flight performance models, the generation of flight profiles, and modeling of the vehicle noise sources based on propulsor characteristics of differing scales. The methodology is then implemented to assess the vehicle's noise, in terms of both noise certification levels, which are evaluated against the Federal Aviation Administration's (FAA's) Stage 5 noise standards [20], as well as single-event noise contours and noise differences in areas beyond the observer locations examined by the Stage 5 noise standards to assess broader community impacts. These are compared to a

Presented as Paper 2024-2105 at the AIAA SciTech 2024 Forum, Orlando, FL, January 8–12, 2024; received 19 March 2024; accepted for publication 31 December 2024; published online 4 February 2025. Copyright © 2025 by Victoria Pellerito, Mallory Mott, Naomi Acosta, Jacqueline Huynh, Jack Ahrens, Franco Staub, Judy Gallman, and John Vassberg. Published by the American Institute of Aeronautics and Astronautics, Inc., with permission. All requests for copying and permission to reprint should be submitted to CCC at www.copyright.com; employ the eISSN 1533-3868 to initiate your request. See also AIAA Rights and Permissions www.aiaa.org/randp.

^{*}Graduate Student, Department of Mechanical and Aerospace Engineering, 4200 Engineering Gateway; vpelleri@uci.edu. Student Member AIAA (Corresponding Author).

[†]Graduate Student, Department of Mechanical and Aerospace Engineering, 4200 Engineering Gateway. Student Member AIAA.

[‡]Undergraduate Student, Department of Mechanical and Aerospace Engineering, 4200 Engineering Gateway. Student Member AIAA.

[§]Assistant Professor, Department of Mechanical and Aerospace Engineering, 4200 Engineering Gateway. Member AIAA.

[¶]Aero Design Engineer, 4150 Donald Douglas Dr, Long Beach, CA 90808.

^{**}Aircraft Performance Engineer, 4150 Donald Douglas Dr, Long Beach, CA 90808.

^{††}Aeroacoustics Engineer, 4150 Donald Douglas Dr, Long Beach, CA 90808. Associate Fellow AIAA.

^{‡‡}Chief Design Officer, 4150 Donald Douglas Dr, Long Beach, CA 90808. Fellow AIAA.

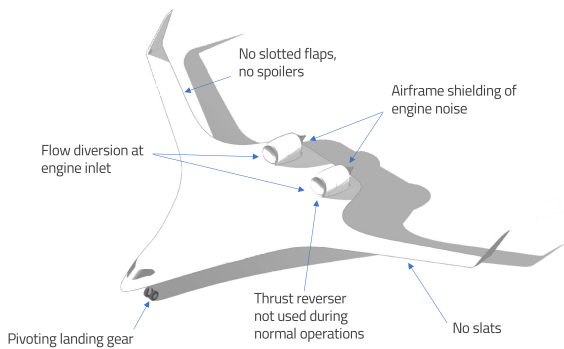


Fig. 1 Representative JetZero BWB aircraft with low-noise features highlighted [4].

reference tube-and-wing aircraft of similar weight and range class. This methodology draws inspiration from BWB configuration acoustic modeling frameworks developed at NASA Langley, with an emphasis on propulsor characteristic variations and their effect on both certification and community noise levels [11,21,22].

This study is performed on a representative BWB twin-engine aircraft under development at JetZero, Inc., shown in Fig. 1 [4]. This BWB aircraft carries approximately 230 passengers. For this study, the fuel load was determined such that the BWB aircraft matches the 4600 nmi range of the A321-XLR. The engines utilized in this study are similar in class to that of the Pratt & Whitney 1100-series Geared Turbofan Engine (PW1100G).

The paper also addresses the unique features of the JetZero BWB. In particular, the low-noise BWB configuration does not include slats, spoilers, or slotted flaps; simple sealed hinge flaperons are deflected 15–25 deg at takeoff and landing conditions. The BWB configuration also features over-centerbody, semiburied engines, mounted aft of the cabin's pressure bulkhead. While the engines are closely coupled with the airframe, the airframe's boundary layer experiences flow diversion away from the engine inlet; hence, flow diversion technology is assumed, with the engine not ingesting the boundary layer. Placement of the engines provides significant shielding of fan noise and partial shielding of aft fan noise. Lastly, this BWB aircraft includes a novel pivoting landing gear, which has the potential to eliminate the need for thrust reversers upon landing. Such characteristics deviate significantly from those of conventional tube-and-wing transport aircraft; thus, this study performs a noise analysis of this BWB aircraft's features and procedure capabilities in comparison to baseline features from standard tube-and-wing aircraft to provide an understanding of the capabilities that a BWB vehicle has in reducing the community noise impact for the aviation industry.

The remainder of this paper is structured as follows: A breakdown of the analysis methodology is described in Sec. III, with the framework for the BWB aircraft performance model, noise model, and the details of the noise assessment provided in Secs. III.A, III.B, and III.C, respectively. The framework is applied to the conceptual BWB vehicle in Sec. IV, where the noise contributions for individual characteristics of the BWB aircraft and noise certification analysis are presented in Sec. IV.A, and flight procedure noise performance and the comparison to a conventional tube-and-wing aircraft are presented in Sec. IV.B. Finally, a summary of the results is presented in Sec. V.

II. Methodology to Assess Flight Procedural Noise of a BWB Aircraft with Variable Engine Thrust

The methodology for modeling the BWB aircraft noise according to the designed approach and departure flight profiles and variable engine thrust is presented in Fig. 2. The framework is composed of a BWB Aircraft Performance Module and a BWB Aircraft Noise Module, of which the details are explained in Secs. III.A and III.B, respectively. The outputs of the framework include the 14 Code of Federal Regulations (CFR) Part 36 certification noise levels, community noise contours of various flight procedures, and a comparison of individual aircraft component noise sources with respect to each other. The flight procedure modeling can be used to assess community noise contours resulting from operational differences, such as speed, configuration, thrust, and altitude. In addition, the methodology can be used to compare the BWB vehicle against traditional tube-and-wing aircraft, such as those with published certification noise levels as well as those modeled in previous studies [19]. The details of such applications and how they are used in this study are described in Sec. III.C.

A. BWB Aircraft Performance Module

The BWB Aircraft Performance Module provides necessary data about the aircraft and its performance characteristics required for the detailed noise source models. This data includes details of the flight profile, such as thrust, velocity, altitude, high-lift devices and landing gear settings per flight phase, internal engine performance, and aircraft geometry. The methods that are used within each module are described below. Utilizing the BWB aircraft characteristics, such as weight, airframe geometry, and flight performance, the Aircraft Performance Module executes both a propulsor design model and flight profile generation model, as depicted in Fig. 2.

The Propulsor Design Model of the modeling framework presented in Fig. 2 consists of an engine thrust model and a Kerrebrock engine state model. The Kerrebrock engine state model [23] is implemented through the use of the Transport Aircraft System Optimization (TASOPT) program, which is a component-based thermodynamic cycle analysis that is used to size the engine for cruise and determine the engine performance at off-design conditions [24]. In this framework, a baseline engine is sized according to the maximum static takeoff thrust, bypass ratio, operating pressure ratio, turbine inlet temperature, and gear ratio to obtain the internal operating states necessary for the noise model. Various design conditions, such as the turbine inlet temperature, can be modified, scaling the engine from the baseline to generate a new propulsion system with a different maximum thrust capability. From a sized propulsor, engine performance states, such as temperatures and pressures, for off-design thrust and Mach number conditions from the flight profile are determined and are outputted to the flight profile generation module and noise model, as shown in the framework in Fig. 2. The engine performance is necessary for determining modified departure and arrival trajectories, which can alter the noise certification assessment described in Sec. III.C.1 and the overall noise contour of a given flight procedure constructed according to the methodology described in Sec. III.C.2. Thus, as a part of this analysis, the tradeoffs of engine design and flight procedure performance are assessed through noise certification data and contour comparisons.

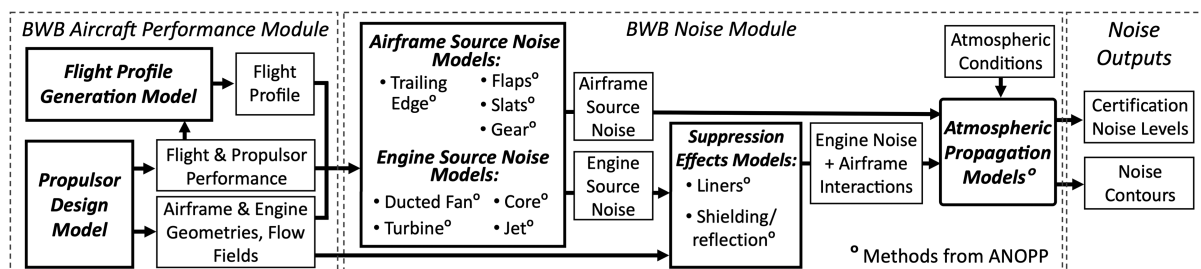


Fig. 2 Flight procedural noise modeling framework for BWB aircraft.

The BWB aircraft flight profiles are generated using a 3-degree-of-freedom, time-stepped approach that employs representative engine, weight, and aerodynamic models. For takeoff trajectories, the engine throttle is declared at each time step based on declared cutback or climb gradient schedules, and a Newton–Raphson trimming algorithm is used to zero out pitching moments [25]. A 5 s spool-up time is applied at the start of the takeoff roll. The on-ground pitch rotation rate does not exceed 3.5 deg per second, and once in the air, the angle-of-attack rate is limited to 3 deg per second. Three seconds after becoming airborne, the landing gear is retracted over a 7 s time period, after which no further configuration changes are made. The landing trajectory is calculated in a similar fashion. The approach path determines thrust and trim deflections. After touchdown, no thrust reversers are used in the low-noise procedure, which is possible due to the increased braking power from the JetZero BWB aircraft pivot landing gear described in Sec. IV.B.2.

B. BWB Aircraft Noise Model

The noise modeling method evaluates the component noise levels for different airframe or propulsor geometries, flight trajectories, and performance of the BWB aircraft at different operational settings. The noise model employed in this methodology is based on the framework for assessing community noise impacts due to tube-and-wing aircraft, as outlined in [19,26]. This model is adapted to assess both BWB performance parameters, relevant to flight procedures, and BWB airframe assumptions, relevant to noise shielding. Airframe geometry and engine states along the flight profile are inputs to NASA’s Aircraft Noise Prediction Program (ANOPP) [27] modules, which are used to assess engine and airframe noise source components.

The engine noise components are assumed to be due to the fan, core, turbine, and jet and vary with the engine state parameters such as turbine inlet temperature and fan rotational speed, as these parameters vary with thrust and velocity along the flight profile. The Krejsa fan noise method of ANOPP is used to assess fan noise [28] for high-bypass-ratio turbofans along with a correction for fan inlet and exit hard-wall acoustic treatment based on a procedure developed by General Electric [29]. The core noise is modeled using the method by Emmerling [30], turbine noise is modeled using the method of Krejsa and Valerino [31], and jet noise with nozzle chevrons is modeled using the Stone method [32].

Airframe noise varies with the flight velocity and high-lift device and landing gear settings along the flight profile, which is determined using the Fink method [33] for wing, vertical, and flap trailing edge noise and Guo methods [34–36] for flap edge, slat, and gear noise, each implemented in ANOPP.

To compare the features of the BWB configuration evaluated in this study to those of standard tube-and-wing aircraft, as mentioned in Sec. II, the modifications of high-lift devices are examined, including slats and slotted flaps. These high-lift devices are modeled using the Guo slat and flap edge models and Fink trailing edge models. Additionally, continuous mold line flaps, which have been shown to reduce radiated flap noise [37], are modeled using the Fink flap trailing edge model only. The landing gear geometry is assumed to be that of the pivot gear of JetZero’s BWB aircraft referenced in Page et al. [4]. Engine noise interactions with the airframe, including noise shielding for overwing-mounted engines and noise reflections for underwing-mounted engines, are assessed with the ANOPP WING shielding method [38] based on Fresnel diffraction theory for a semi-infinite barrier. The surface assumed to impact the engine noise shielding is the fuselage centerbody, as shown in Fig. 3. A study assessing the noise of a representative hybrid wing–body based on the SUGAR Ray concept [39] found that predictions using the ANOPP WING module showed flyover and sideline noise levels to be 2.8 and 5.8 dB higher, respectively, than those predicted using NASA’s Fast Scattering method to model the shielding effect [40]. The WING module allows for rapid yet conservative predictions for BWB configuration noise. Given engine and airframe noise sources, the total noise is propagated to the ground to determine community noise effects at the desired observer locations. Aircraft noise source is

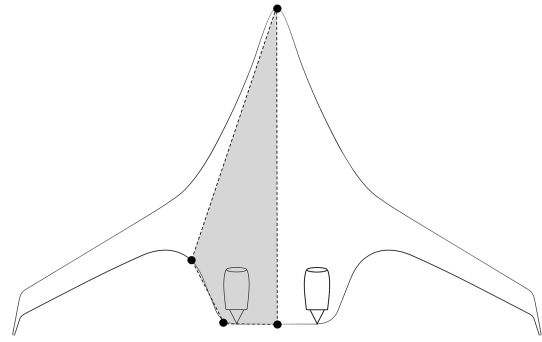


Fig. 3 Area assumed in modeling engine noise shielding by the BWB aircraft centerbody (shaded in gray).

determined throughout the flight profile and is broken into emission time elements. Given the aircraft altitude, the propagation of the aircraft noise source to ground observers is modeled assuming spherical spreading and acoustic impedance in the atmosphere using the SAE ARP 866 atmospheric attenuation method [41]. Sound intensity corrections due to destructive interference of reflecting sound waves when the aircraft is near the ground [42], as well as lateral attenuation due to engine installation, absorption of the ground surface, and refraction and scattering of sound waves when the aircraft is near the ground using the SAE AIR 5662 method [43], are also applied. Noise levels at the ground in various metrics, such as the maximum A-weighted sound pressure level ($L_{A,max}$), tone-corrected perceived noise level (PNLT), and effective perceived noise level (EPNL), can be determined.

C. Output Noise Assessments

The performance and noise modeling methodologies presented in Secs. III.A and III.B are implemented to assess the impacts that various BWB configuration characteristics have on certification noise levels and to generate noise contours used to assess operational impacts on noise performance. These results will be compared to conventional tube-and-wing aircraft of similar weight class, as described in Sec. II.

1. Certification Noise Level Comparisons

The FAA noise certification requirements that are provided in the 14 CFR Part 36 [44] are applied to the various BWB aircraft designs. The certification process includes noise level points from three reference points for three specific flight procedures that are summarized in Fig. 4.

The certification noise levels consist of measurements at the flyover, lateral, and approach reference points depicted in Fig. 4. The measurements for these reference points are obtained during three distinct certification tests, including two departure procedures, all of which are required to be flown at maximum takeoff weight, with high-lift devices in the takeoff setting, at a speed of 10 knots over the takeoff safety speed (V_2), and with the landing gear up. The departure procedures begin operation at maximum thrust, with the flyover reference point requiring a thrust cutback to maintain a 4% climb gradient, or alternatively, a thrust cutback no lower than the one engine inoperative steady flight thrust level, whichever is greater,

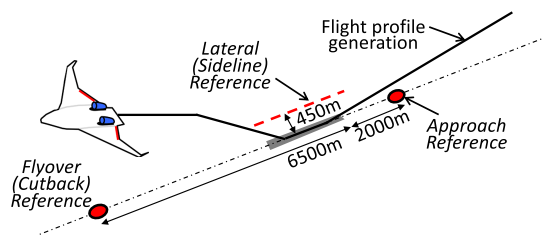


Fig. 4 Certification locations and flight procedure assessed for the BWB aircraft.

performed at an altitude of 300 m. The noise is measured at 6500 m ground track from the start of the takeoff roll. The noise for the lateral reference point is the maximum noise level 450 m lateral to the takeoff track. The approach reference point is measured 2000 m before touchdown on a 3 deg glideslope with the aircraft at maximum landing weight, with high-lift devices in the landing setting, at a speed of $V_{REF} + 10$ knots, and landing gear down. In addition to assessing the certification points, the cumulative EPNLs relative to the FAA Stage 5 noise standards [20] are determined. The lateral, flyover, approach, and cumulative noise levels and margins relative to the FAA Stage 5 standards [20] or, equivalently, the International Civil Aviation Administration's Chapter 14 standards [45] are compared to publicly available noise certification data of a common tube-and-wing aircraft, where the margin is the amount of decibels below the limit for the number of engines and aircraft weight.

2. Community Noise Contours on Approach and Departure Comparisons

The standard procedures described in Sec. III.C.1 are valuable for certification guidelines but fall short in the assessment of full community noise impacts. For example, on departure, noise levels for operational changes beyond 6500 m from the runway cannot be measured with the certification flyover point. In addition, noise levels for operations near the runway on final approach, such as the removal of thrust reversers, cannot be assessed with the certification approach point. In order to examine the community noise impacts of a complete approach or departure procedure and variations in the procedure design, observer noise levels at regions beyond the certification

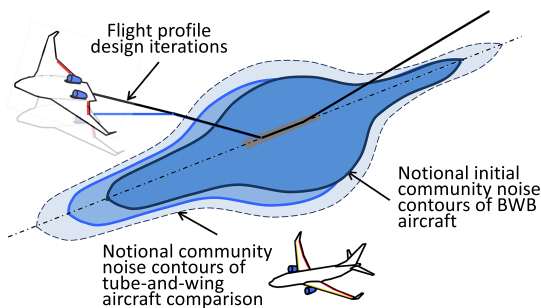


Fig. 5 Conceptual visualization of flight procedure noise contour comparisons.

Table 1 Reference and modeled effective perceived noise levels of the reference tube-and-wing, 2000s technology configuration

Aircraft	Flyover (EPNdB)	Lateral (EPNdB)	Approach (EPNdB)
Boeing 737-800 (2000s Technology [51])	86.7	93.1	96.8
Modeled Boeing 737-800	89.2	94.0	98.0

locations must be considered. With the noise source of a given aircraft and the flight profile generated according to the framework presented in Fig. 2, propagation of noise is modeled from the source to the ground observer over the entire flight profile. The resulting noise contours provide insight as to how the observer noise changes throughout the full range of operating conditions in a given procedure. By displaying noise contours or differences in noise levels over aerial maps of areas surrounding airports, the community noise impact for the aircraft configuration and flight procedure can be assessed. In addition, noise levels can also be compared to representative tube-and-wing aircraft, such as presented in Fig. 5.

In this study, reference tube-and-wing aircraft noise levels are referenced from approach and departure noise levels of year 2000 technology, Boeing 737-800 with CFM56-7B/26 engines. This configuration was chosen for comparison because it is a market-dominating vehicle and is a reference for industry goals being recommended by agencies such as the NASA N+3 goals [46] and the European Union Advisory Council for Aviation Research's Flight Path 2050 initiative [47]. For the results shown in this paper, the drag performance of the reference tube-and-wing aircraft for different configurations is obtained from [48], while takeoff safety speed (V_2) and reference speed (V_{REF}) are obtained from the Boeing 737-800 operations manual [49]. The CFM56-7B/26 engine states were modeled using the same Kerrebrock engine state model as described in Sec. III.A, while the noise levels were determined using the same noise models as those described in Sec. III.B with the exception of the fan noise, which was modeled using the Heidmann large fan method [50] (as it was developed incorporating CFM56 engine data). Results of the modeling method for the Boeing 737-800 flying the 14 CFR Part 36 procedures were compared to publicly available noise certification data [51] and are shown in Table 1. The modeled noise levels are between 0.9 and 2.5 EPNdB louder than the published noise levels, indicating fair agreement for the modeling method.

III. Demonstration of Methodology on Example BWB Aircraft

The flight procedure design and noise analysis methodology summarized in Sec. III is implemented on a BWB, representative of the JetZero vehicle (see Sec. II and Fig. 1) [4]. To analyze the impact that individual aircraft characteristics have on the noise of the vehicle, multiple variations of the BWB vehicle are studied against the noise certification analysis described in Sec. III.C.1 and the noise contours described in Sec. III.C.2. A summary of the features that are being studied is presented in Fig. 6.

The noise certification analysis is performed on a baseline aircraft featuring the BWB airframe with underwing-mounted engines and high-lift devices, including slats and flaps with side edges, as well as modified BWB aircraft with engine shielding, flow diversion, and simplified high-lift devices. The results of these comparisons are included in Sec. IV.A. The lowest noise variation of the BWB configuration with engine shielding, flow diversion, and high-lift device modifications is then compared with PW1100G class engines resized in the Propulsor Design Model with varied maximum thrust

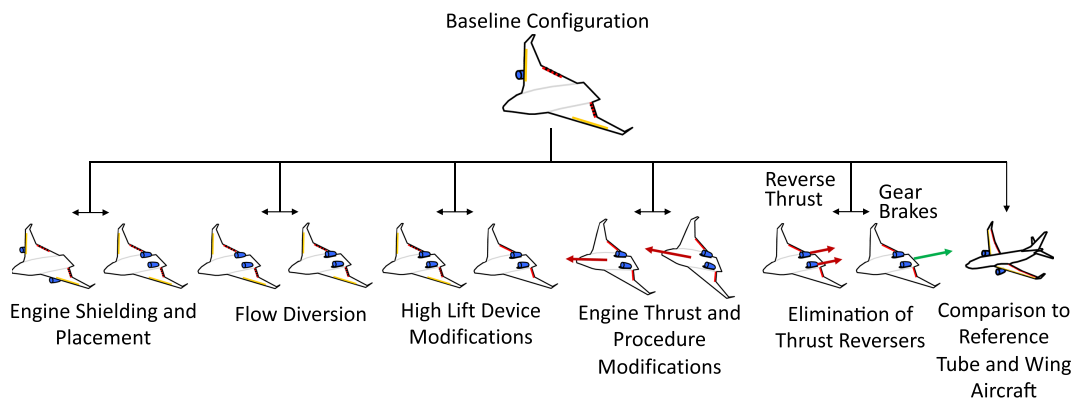


Fig. 6 Assessment criteria for noise of individual characteristics of BWB aircraft design and procedure.

capabilities in Sec. IV.A.2. Additionally, a comparison of the BWB aircraft takeoff and landing performance and single-event community noise contours is provided and compared to a reference tube-and-wing aircraft, the Boeing 737-800. This also includes a demonstration of the aircraft’s landing gear braking capabilities and the corresponding noise reduction compared to the use of thrust reversers in Sec. IV.B.2.

A. Noise Contributions for Individual Characteristics of BWB Aircraft Configuration

To assess the individual contributions to the 14 CFR Part 36 [44] noise certification requirements, three BWB aircraft flight procedures were constructed according to the methodology described in Sec. III.A that follow the noise certification procedures described in Sec. III.C.1. The three profiles presented in Figs. 7a–7c demonstrate the procedures necessary to provide the flyover, lateral, and approach noise assessments, respectively.

1. Noise Certification Results for Engine Shielding, Flow Diversion, and High-Lift Devices

The noise certification analysis described in Sec. III.C.1 is performed on a baseline configuration of the BWB, including slats, slotted flaps, and underwing engine installation similar to conventional commercial transports. The potential contribution to the noise levels of boundary-layer ingestion (BLI) is also evaluated. The same analysis is then performed on modified configurations that include engine shielding, flow diversion, and high-lift device modifications as presented in Fig. 6. In doing so, this demonstrates the noise reduction capabilities of each characteristic of the BWB vehicle.

With the established performance capabilities of the aircraft, noise analysis of the given configuration is done according to the methods presented in Sec. III.B. First, the baseline configuration that is most comparable to a traditional tube-and-wing aircraft is assessed at the certification points to provide baseline results to compare the improved BWB vehicle characteristics against. This baseline configuration was assumed to have underwing-mounted engines exposed to the freestream, from which the engine noise is reflected from the underside of the wing, and complex high-lift devices.

The analysis is then performed on a series of changes until converging on the nominal BWB configuration, resembling that of the JetZero configuration presented in Fig. 1. Figure 8 shows the tone-corrected perceived noise levels for the baseline configuration of the BWB aircraft evaluated at the certification locations described in Sec. III.C.1, including a flyover, lateral, and approach point. Shown in Fig. 9 is EPNL distribution for each certification point. Of note, the lateral noise measurement was maximum when the aircraft reached an altitude of approximately 170 feet. The results indicate that baseline aircraft noise is dominated by the fan in the flyover and lateral certification points. In addition, the slat noise is dominant on approach.

To examine engine positioning that resembles the JetZero BWB configuration, the engines are modified to an overwing mounting. This also implies that the engine noise will be shielded, which is included in the noise model as described in Sec. III.B. Shielding is applied using the ANOPP wing shielding method, where attenuation is applied to sound waves from the engine that intersect with the aircraft body before radiating to the observer, assuming the shielding surface represented in Fig. 3.

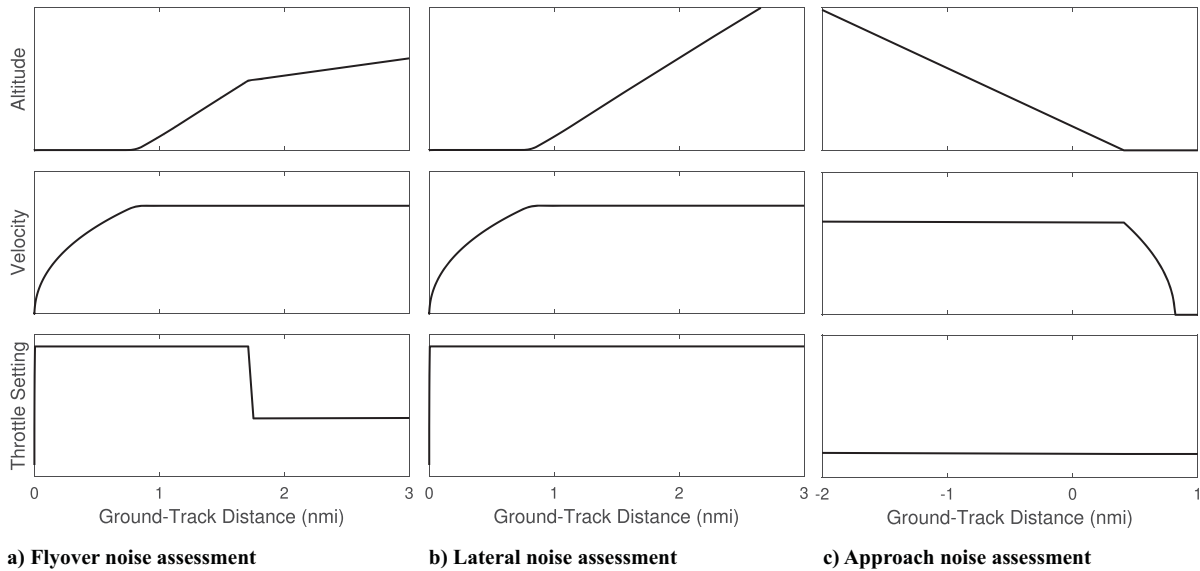


Fig. 7 Flight profiles of BWB aircraft noise certification analysis.

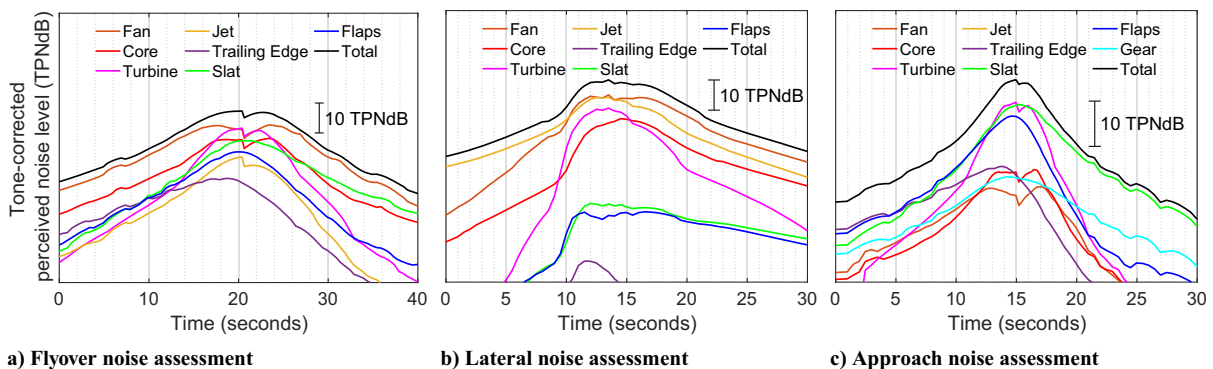


Fig. 8 Tone-corrected perceived noise levels during flyover, lateral, and approach for baseline configuration, including underwing engines and complex high-lift devices.

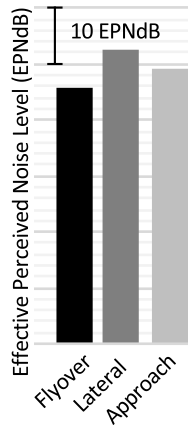


Fig. 9 Effective perceived noise level distribution during flyover, lateral, and approach for underwing engine shielding and complex high-lift devices.

As described in Sec. II, a feature of the JetZero BWB aircraft in this overwing-mounting configuration is the implementation of flow diversion of the boundary layer that develops over the top surface of the aircraft body as opposed to BLI into the engines. To estimate the impacts due to BLI, if implemented, the relative contribution to the overall noise due to the fan is evaluated in comparison to the other noise source levels. BLI at the inlet of an aircraft's engine is known to increase broadband and tonal fan noise as a result of uneven loading of the fan blades. Estimations of the impacts of BLI on fan noise and resulting certification noise levels for aircraft have been studied previously, such as in the work of Clark et al. [52], which presents an acoustic model that shows increases in both broadband and tonal noise sources due to turbulence ingestion into the fan. In the model proposed by Clark et al. [52], tonal fan noise levels were shown to increase by around 5–14 dB, depending on the polar angle fore and aft of the engine, with the inclusion of BLI, while broadband noise levels were shown to increase between 0 and 8 dB. From this work, for demonstration, a reference average increase in noise level of 7 dB above modeled peak fan noise source levels determined from the Kreja model is used to estimate the potential effects due to BLI. This effect would be significant in cases where the fan noise is a dominating noise component.

The resulting noise distributions, assuming shielding as well as flow diversion instead of BLI, are presented in Figs. 10 and 11, with the same vertical scales as the baseline results in Figs. 8 and 9. The resulting noise levels suggest that the BWB aircraft with overwing engines has a notable decrease in engine noise source levels at each of the certification points. The fan noise continues to be the dominating noise source in the lateral certification point, while the slat noise becomes the dominant noise source during the flyover and remains dominant during the approach. The effects of flow diversion rather than ingesting the boundary layer can be discerned from the noise results. Examining the noise source distributions, because

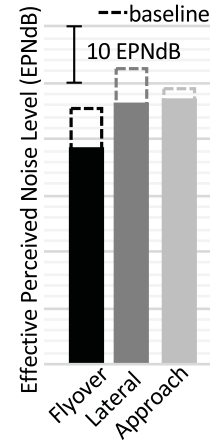


Fig. 11 Effective perceived noise level distribution during flyover, lateral, and approach for overwing engine shielding, flow diversion, and complex high-lift devices, including comparison to the baseline.

of the high fan noise source levels in comparison to other sources, noise due to BLI would be expected to still contribute significantly to the flyover and lateral points even with attenuation due to engine noise shielding.

The final noise reduction characteristic assessed in this noise certification analysis is the simplification of high-lift devices. The sealed flaperons of the BWB aircraft reduce the noise sources of the airframe by eliminating gaps and edges. The baseline configuration, of which noise certification results are presented in Figs. 8 and 9, includes conventional slats and flap edge noise that are eliminated to result in the complete low-noise BWB configuration. The tone-corrected perceived noise levels and EPNLs for the low-noise BWB configuration with simplified high-lift devices, flow diversion, and overwing-mounted engines are presented in Figs. 12 and 13, respectively. As the BWB vehicle does not have slats and relies entirely on the sealed flaperons for control, the slat noise is eliminated entirely. The sealed flaperons provided flap noise reductions at each of the flyover, lateral, and approach certification points, respectively. It should be noted that the 8.0 TPNdB reduction of the peak flap noise and removal of slat noise on the lateral certification point resulted in negligible reductions of total noise, as it is not the primary noise source. However, a more significant reduction was noted for the flyover and approach points because airframe noise was previously the dominant noise source.

The results in Fig. 13 are those of the final configuration of the BWB. The elimination of slat noise results in fan noise being the dominant noise source for the flyover and lateral certification points, while the flap noise is the dominant noise source for the approach point. The total EPNLs have decreased by a minimum total of 12.0, 6.3, and 9.5 EPNdB for the flyover, lateral, and approach certification points from the original baseline configuration results in Fig. 9, with the effect expected to be greater for the flyover and lateral

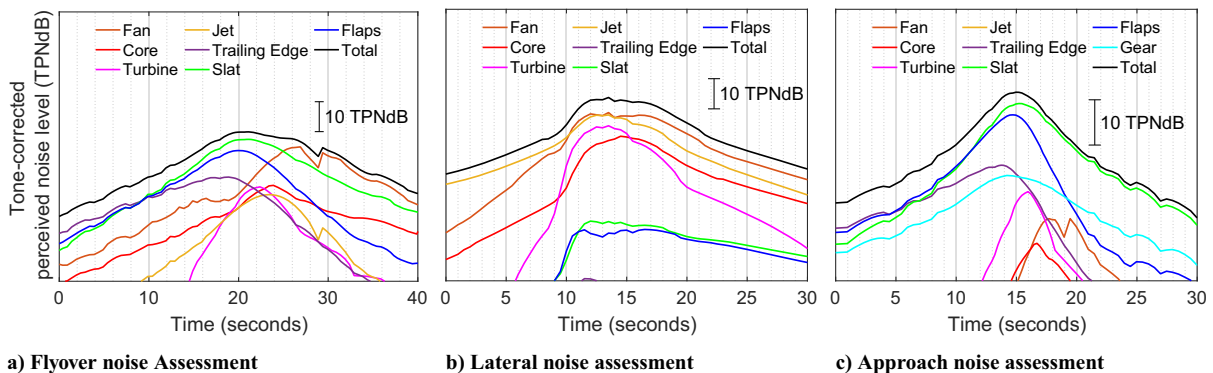


Fig. 10 Tone-corrected perceived noise levels during flyover, lateral, and approach for baseline configuration, including overwing engine shielding, flow diversion, and complex high-lift devices.

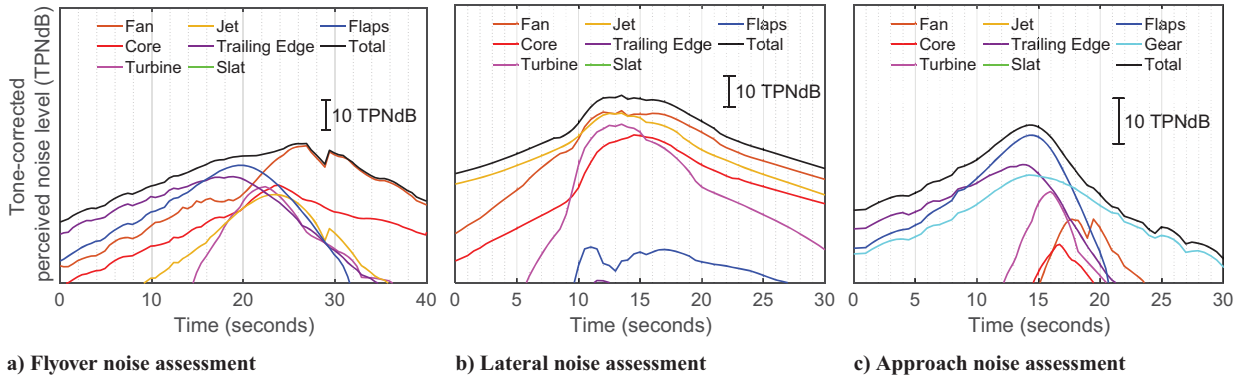


Fig. 12 Tone-corrected perceived noise levels during flyover, lateral, and approach for baseline configuration, including overwing engine shielding, flow diversion, and simplified high-lift devices.

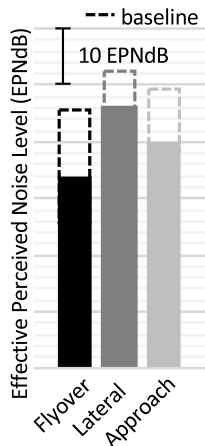


Fig. 13 Effective perceived noise level distribution during flyover, lateral, and approach for overwing engine shielding, flow diversion, and simplified high-lift devices, including comparison to the baseline.

certification points if BLI was assumed as opposed to flow diversion. The cumulative EPNLs of the final BWB configuration modeled are summarized in comparison to the published levels of the Boeing 737-800 with CFM56-7B engines, relative to Stage 5, in Table 2. The margin to Stage 5 shown in Table 2 is determined according to the certification process as described in Sec. III.C.1.

Relative to Stage 5, or equivalently 17 EPNdB below Stage 3 of the FAA standards [20], the Boeing 737-800 with CFM56-7B engines is 4.0 EPNdB above the standard according to published certification noise levels, whereas the BWB configuration studied is 35.8 EPNdB below the standards. It should be noted that part of the difference can be attributed to the Boeing 737-800 featuring engines with year 2000 technology. Thus, this BWB configuration is quieter than the present-day equivalent transport vehicle and greatly satisfies the most relevant noise standards. These results are consistent with trends observed in assessments by both NASA and the German Aerospace Center, which demonstrates the significant advantages of BWB aircraft over tube-and-wing designs, even when integrating different engines into the BWB aircraft model [11] [3]. The findings additionally complement the recent NASA study on noise reduction via alternative aircraft configurations, which supports that, given current technology development, the hybrid wing-body aircraft type is the most viable option for achieving

the long-term noise goals outlined in the Aeronautics Research Mission Directorate’s 2019 Strategic Implementation Plan [40].

2. Noise Certification Results for Variable Engine Maximum Thrust Study

The low-noise BWB configuration, with the results presented in Fig. 13, is compared against different variations of the vehicle with PW1100G-class engines. The baseline engine design turbine inlet temperatures were adjusted to result in engines with the same fan diameter but with different maximum thrust capabilities: one with an increased takeoff thrust compared to the baseline and one with a decreased thrust compared to the baseline. Off-design engine maps for each design were obtained to determine the propulsor performance states for the flight profiles and engine component noise levels. By modifying the design of the baseline engine using the methodology described in Sec. III.A, the overall takeoff performance of the vehicle changes. Increasing the maximum takeoff thrust increases the climb rate and increases engine noise. Therefore, this tradeoff may result in variations in the noise certification results. The certification procedures were modeled for both the increased and decreased takeoff thrust case using the method described in Sec. III.C.1, and the component noise breakdown was assessed in the same manner as the previous section. Figure 14 presents the flight profiles of the noise certification procedures for the different engine variants.

As seen in Fig. 14, the different maximum takeoff thrust ratings of the engines result in different climb rates for the two takeoff procedures, and thus there are different cutback locations for the flyover noise assessment procedure. Note that the approach noise assessment procedure remains unchanged, as this procedure relies on the required thrust to maintain the 3 deg descent angle. The resulting EPNLs for the modified engine variants are summarized in Table 3, where the baseline is the final BWB configuration of Sec. IV.A, the results of which are presented in Fig. 13 and Table 2.

The results indicate that the cumulative total EPNL is reduced by 2.0 EPNdB with the decreased engine rating and increased by 1.6 EPNdB when the engine rating is increased. The best margin to Stage 5 is with the decreased maximum takeoff thrust engine at 37.8 EPNdB below the standards.

B. Departure and Arrival Procedure Comparison

The design of a given aircraft and the procedure flight go hand in hand with respect to the overall community noise impact of an aircraft. Thus, various studies were executed to understand the capabilities of the BWB aircraft, and the resulting noise impacts of different procedures are shown and compared to conventional tube-and-wing aircraft for

Table 2 Effective perceived noise level margins of the BWB low-noise configuration compared to reference tube-and-wing configuration

Aircraft	Flyover (EPNdB)	Lateral (EPNdB)	Approach (EPNdB)	Cumulative total (EPNdB)	Margin to Stage 5 (EPNdB)
Boeing 737-800 (2000 Technology)	5.2	3.9	3.9	13.0	-4.0
BWB low-noise configuration	19.4	11.6	21.8	52.8	35.8

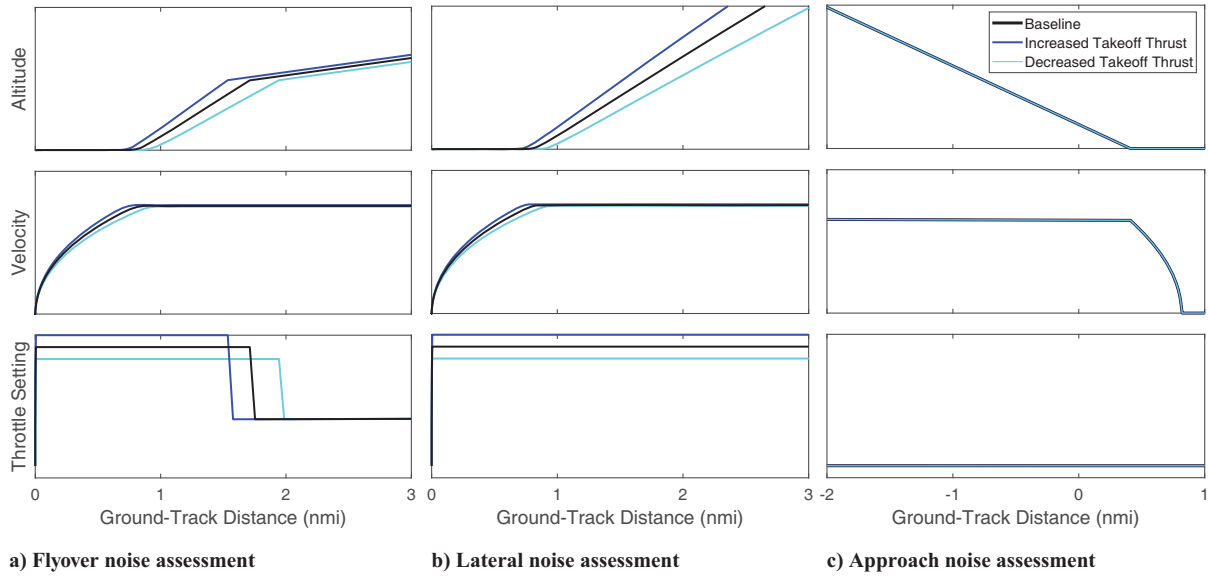


Fig. 14 Flight profiles of noise certification procedures for engine sizing study.

Table 3 Effective perceived noise level margins of the BWB low-noise configuration for various engines of the PW1100 class

Engine variant	Flyover (EPNdB)	Lateral (EPNdB)	Approach (EPNdB)	Cumulative total (EPNdB)	Margin to Stage 5 (EPNdB)
Decreased	19.8	13.2	21.8	54.8	37.8
Baseline	19.4	11.6	21.8	52.8	35.8
Increased	19.1	10.3	21.8	51.2	34.2

departure and arrival procedures in Secs. IV.B.1 and IV.B.2, respectively, using the framework described in Secs. III.B, III.C, and III.D for both the BWB aircraft and the baseline tube-and-wing aircraft. The sound level contour analysis for these cases is focused on the examination of the 60 dB $L_{A,max}$ level, where aggregate procedures align with community annoyance for concentrated flight tracks [53]. Lastly, in Sec. IV.B.2, the novel pivoting landing gear of the JetZero BWB, which can potentially eliminate the need for thrust reversers, is examined to understand the noise reduction impact of this component of the vehicle.

1. Comparison of Example Departure Procedures to Conventional Tube-and-Wing Aircraft

Observer noise is not only a function of an aircraft's performance and airframe characteristics but is also dependent on the flight trajectory of the vehicle. However, the impact that procedural changes have on the observer noise is not fully represented by the certification data studied in Sec. IV.A alone. This is because the procedural changes typically occur at larger distances from the airport than what is conveyed by the certification points. Thus, although the certification noise results of Sec. IV.A show that the BWB vehicle is significantly quieter than the conventional tube-and-wing aircraft as well as the most recent certification standards, the BWB vehicle can be further examined to understand what low-noise procedures for BWB vehicles look like and how quietly the vehicle can operate.

To build an understanding of the impact that operational changes have on observer noise of the BWB vehicle, a study comparing single-event noise contours is performed on a sweep of cutback departure procedures. The results are compared against each other, and a sample procedure is compared to a reference tube-and-wing aircraft, the Boeing 737-800, operating at 85% MTOW. The BWB vehicle performs a maximum thrust departure at 85% MTOW, following a similar takeoff weight percentage to that of the Boeing 737-800 procedure. A thrust cutback is performed at 300 m to different percent maximum thrusts, as displayed in Fig. 15a. As indicated in the figure, the increased cutback percentage indicates, for example, that maintaining 100% is considered a 0% cutback, whereas increasing the cutback

percentage by 20% would result in operating at 80% throttle. The level at which the cutback is performed alters the climb rate of the vehicle, as well as the acceleration rate, as shown in Fig. 15a. However, although a higher throttle setting results in a higher climb rate, the engine is operating at a higher setting, which typically results in more engine noise source. Thus, these tradeoffs are studied by comparing the resulting 60 dB $L_{A,max}$ single-event noise contours, as presented in Fig. 15b with the aircraft departing from Seattle Tacoma International Airport (KSEA). It should be noted in these examples that the SAE AIR5662 lateral attenuation correction is not applied for the $L_{A,max}$ levels, resulting in potentially higher predicted sound levels for observers when the aircraft is closer to the ground. These resulting noise contours indicate that performing cutback procedures is beneficial for BWB aircraft noise, as a general trend of decreasing contour area with increasing cutback percentage can be seen in Fig. 15b. Thus, implementing flight procedures with an increased cutback percentage can have lower noise levels on takeoff for the BWB vehicle studied.

A representative BWB vehicle departure procedure from Fig. 15 is compared to a standard Boeing 737-800 departure procedure. In the Boeing 737-800 departure procedure, the thrust was modeled such that the aircraft's climb angles matched mean departure from flight radar data presented in [19]. Aside from the initial higher throttle setting, the modeled BWB aircraft cutback procedure presented in this study mimics the Boeing 737-800 procedure, as shown in Fig. 16a. In comparison, the BWB vehicle procedure has a shorter takeoff field length, and the thrust cutback occurs approximately 0.5 nmi earlier. However, the Boeing 737-800 reaches climb velocity sooner and maintains a lower throttle setting through the remaining procedure. The resulting 60 dB $L_{A,max}$ single-event noise contours, presented in Fig. 16b, indicate that the overall area and extent of the BWB aircraft contour are significantly smaller than that of the Boeing 737-800.

2. Comparison of Example Arrival Procedures to Conventional Tube-and-Wing Aircraft

Similar to the previous section on departure procedures, the single-event noise contour of an arrival procedure is compared to a reference

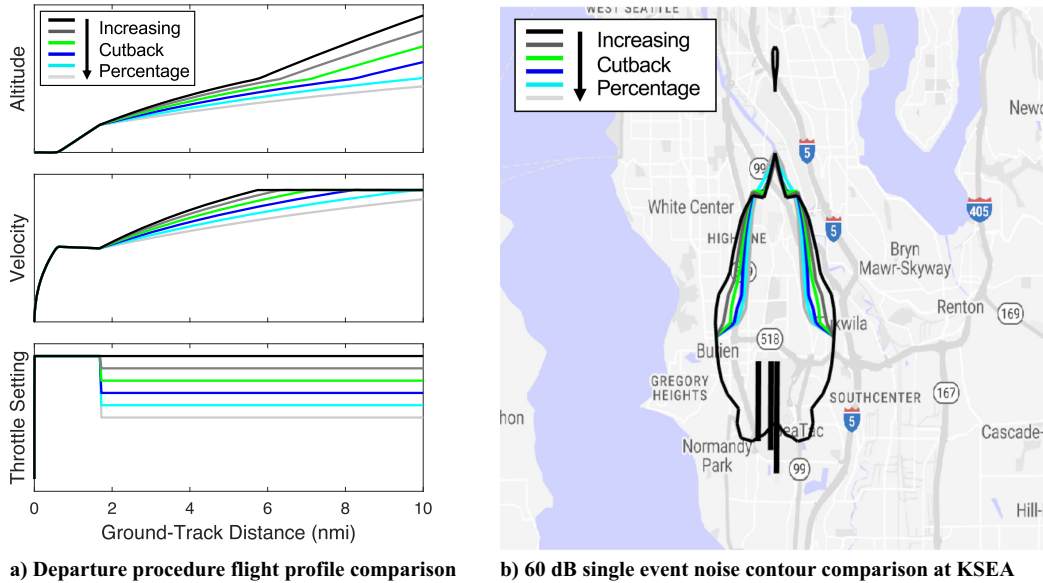


Fig. 15 BWB aircraft flight performance and noise comparison of departures with multiple thrust cutback profiles.

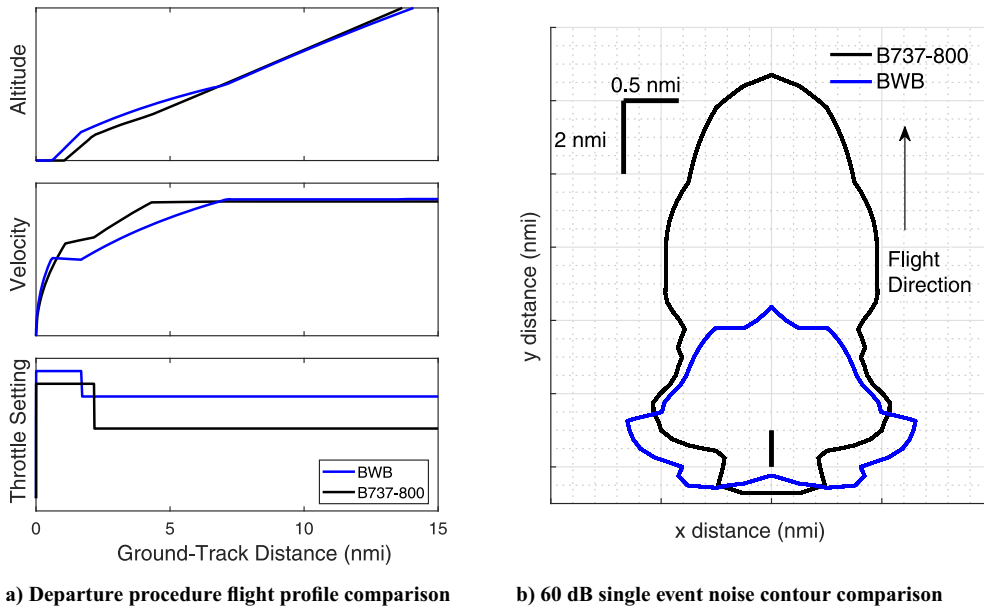


Fig. 16 Flight performance and noise comparison for a BWB aircraft departure compared to the Boeing 737-800.

tube-and-wing aircraft, the Boeing 737-800, following a 3° descent procedure resembling flight radar approach data as referenced in [19]. In this case, both the Boeing 737-800 and BWB aircraft are operating at their respective maximum landing weights. The flight profile for each of the procedures and the corresponding contours are displayed in Figs. 17a and 17b, respectively.

In this case, the two vehicles perform similar flight profiles, but due to the BWB aircraft’s ability to operate at a lower velocity due to its lower wing loading along with the simplified high-lift devices, it has a drastically reduced single-event noise contour at less than 1/4 the along-track distance. The slats, slotted flaps, and flap edge noise that are present in the Boeing 737-800 high-lift configurations and their early deployment of them, based on the flight radar data studied in [19], result in a significant difference in the 60 dB single-event noise contours of the two aircraft while performing similar procedures. Additionally, the Boeing 737-800 is required to operate at a higher throttle setting and at a higher velocity, which respectively increases engine and airframe noise. The same 3 deg angle arrival procedure of the BWB vehicle is performed at John Wayne International Airport (KSNA), and the 60 dB $L_{A,max}$ single-event noise contour is plotted in

Fig. 18. This difference is expected to be less dominant in a time-based single-event metric such as sound exposure level; however, the differences are in agreement with the differences observed in the EPNL results from Sec. IV.A.1.

Lastly, the JetZero BWB vehicle’s novel pivoting landing gear, illustrated in Fig. 19, yields an additional braking force due to the position of the center of gravity and the resulting load distribution on all three landing gears compared to a traditional tricycle configuration. This eliminates the need for thrust reversers upon landing [4].

The resulting impacts of this feature are not observable in the noise certification results of Sec. IV.A. Thus, in order to demonstrate the noise level impacts that this system has on the overall noise of the vehicle, a landing procedure is performed both with and without the use of thrust reversers (see Fig. 20a). The resulting reduction in $L_{A,max}$ noise at two sideline locations when the aircraft performs its landing roll on the runway is shown in Fig. 20b.

As shown in Fig. 20b, replacing the need for thrust reversers through the use of the pivot gear braking system results in a reduction of the noise contour during the ground roll on the runway that extends to the sideline. This indicates the possibility for not only a quiet final

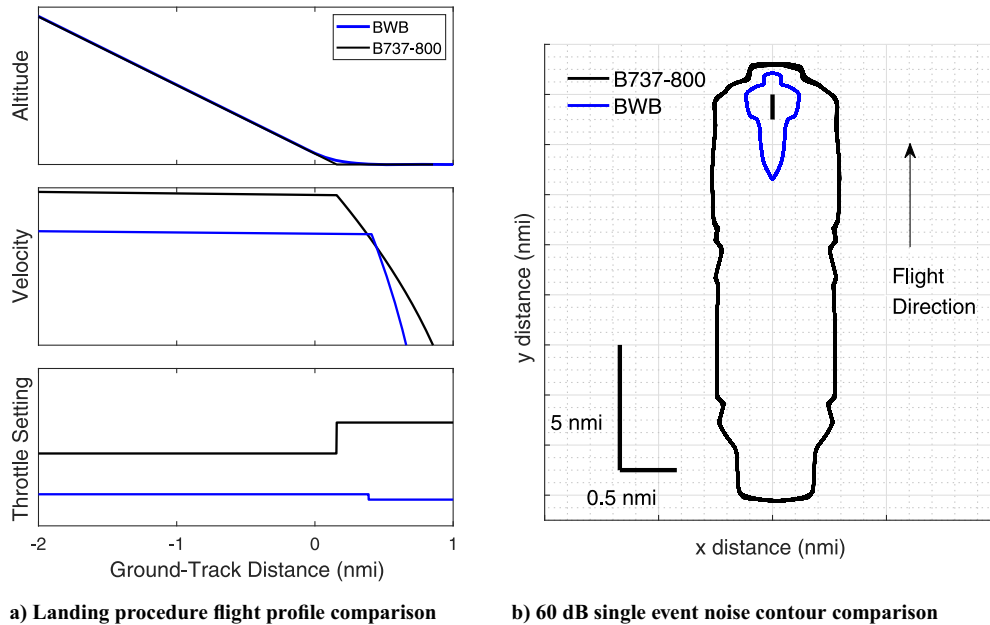


Fig. 17 Flight performance and noise comparison of a BWB aircraft landing procedure compared to the Boeing 737-800.

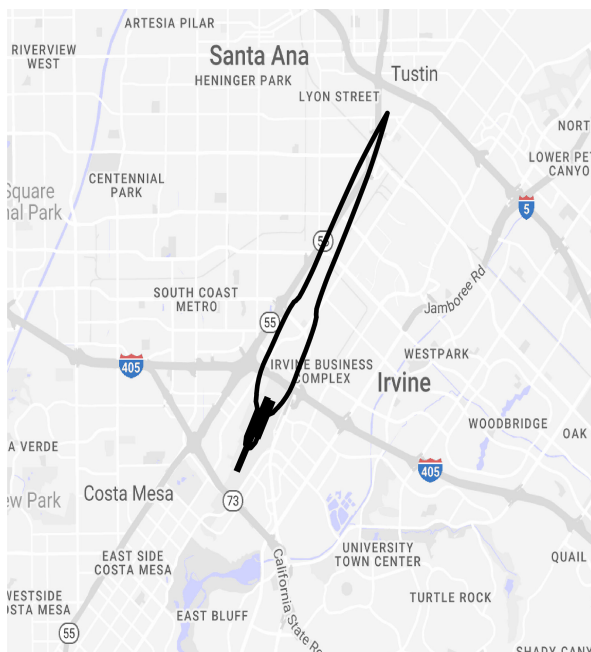


Fig. 18 The 60 dB single-event noise contour of BWB aircraft during a 3 deg descent arrival at KSNA.

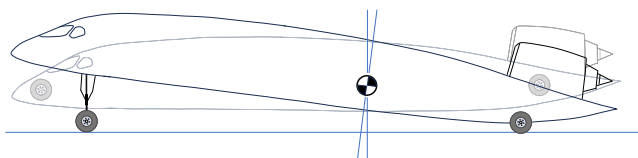


Fig. 19 Illustration of JetZero pivot gear technology [4].

approach but also minimal noise impacts when the BWB aircraft has landed for both onboard passengers and local communities or businesses residing close to the airport.

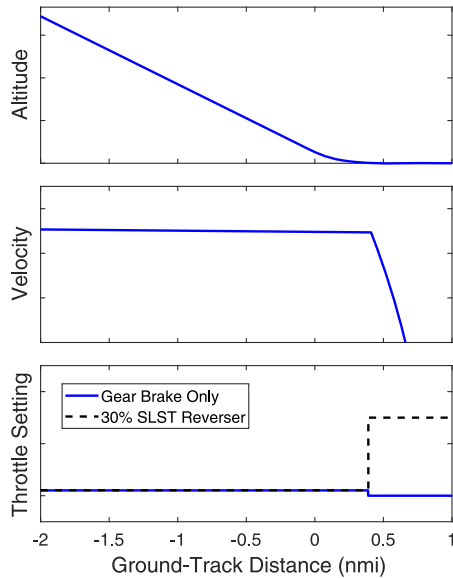
IV. Conclusions

The investigation discussed in this paper presents the opportunity to reduce noise pollution in communities surrounding BWB aircraft.

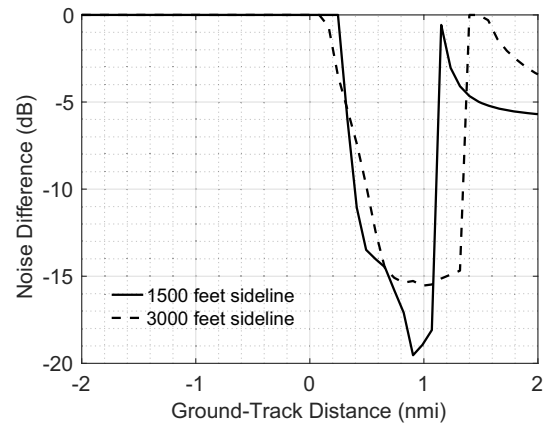
The analysis in this study uses methods for modeling noise source assessments and noise contours based on flight performance data generated by models of engine operations and flight profile characteristics. The propulsion design model enables the evaluation of the effects of maximum thrust capability on the aircraft, as well as the engine performance at off-design conditions. The flight profile model allows the analysis of flight procedure conditions, focusing on take-off and landing trajectories as they are significant to community noise. To assess the noise pollution corresponding to a conventional tube-and-wing aircraft and various operational settings of the BWB configuration, the noise model integrates data generated in both the engine and flight profile models.

The noise analysis framework assesses engine and airframe noise source components, including characteristics unique to the BWB vehicle. The application of such models generates noise data for both the 14 CFR Part 36 certification points and the aerial community noise contours around airports, supporting the requirements necessary and considering a more informed view beyond those reference points. The component breakdown shows that engine noise is an important factor for the lateral condition, whereas airframe noise is the most pertinent factor for approach conditions. Significant noise reduction is observed by engine noise shielding and the implementation of flow diversion, while simplified high-lift devices result in considerable reductions of airframe noise, which is particularly noticeable during the approach. The engine noise and shielding characteristics identified in this study are consistent with the results previously reported by the German Aerospace Center, reinforcing the potential for BWB aircraft to significantly reduce noise impact. Taking into account the BWB low-noise configuration, the model is compared to a Boeing 737-800 in departure and landing trajectories at KSEA and KSNA, respectively. Examination of the community noise contours shows a significant decrease in the affected area for the BWB configuration in comparison to a conventional aircraft configuration, while further reductions in the contour area are observable through additional modifications to the standard departure and arrival procedure operations. These results align with relevant NASA studies previously referenced, which also utilize ANOPP for noise assessment and observe noise footprint area reductions with BWB aircraft takeoff and approach flight paths.

This study establishes a foundation for further advancement in noise reduction technology, particularly in consideration of the BWB aircraft. Moreover, the noise analysis framework is adaptable to multidisciplinary design optimization models, enabling further investigation of noise-reducing strategies in the preliminary phases of the BWB aircraft design process.



a) Landing procedure flight profile comparison



b) Noise reduction at sideline observers of thrust reverser landing roll compared to pivot gear braking landing roll

Fig. 20 Flight performance and noise comparison of a BWB aircraft landing with and without novel reverse thrust capabilities.

Acknowledgment

This study was funded in part by the United States Air Force Defense Innovation Unit. Opinions, interpretations, conclusions, and recommendations are those of the authors and are not necessarily endorsed by the United States Government.

References

- [1] Thomas, J., Li, C., Toscano, P. M. M., and Hansman, J., "Advanced Operational Procedure Design Concepts for Noise Abatement," *13th USA/Europe Air Traffic Management Research and Development Seminar*, Eurocontrol and the Federal Aviation Administration, 2019, http://www.atmseminar.org/seminarContent/seminar13/papers/ATM_Seminar_2019_paper_49.pdf.
- [2] Wienke, F., Bertsch, L., Blinstrub, J., Iwanitzki, M., Balack, P., and Häßy, J., "System Noise Assessment of Conceptual Tube-and-Wing and Blended-Wing-Body Aircraft Designs," *AIAA Aviation 2023 Forum*, AIAA Paper 2023-4170, 2023, <https://doi.org/10.2514/6.2023-4170>.
- [3] LeGriffon, I., Bertsch, L., Centracchio, F., and Weintraub, D., "Flyover Noise Evaluation of Low-Noise Technologies Applied to a Blended Wing Body Aircraft," *INTER-NOISE and NOISE-CON Congress and Conference Proceedings*, Vol. 265, Institute of Noise Control Engineering, Glasgow, Scotland, U.K., 2023, pp. 1305–1316, <https://hal.science/hal-03927942>.
- [4] Page, M., and Vassberg, J., "BWB Enabling Technologies," *33th ICAS Congress 2022*, International Council of Aeronautical Sciences, Stockholm, Sweden, 2022, https://www.icas.icas_ARCHIVE/ICAS2022/data/papers/ICAS2022_0392_paper.pdf.
- [5] Liebeck, R., "Blended Wing Body Design Challenges," *AIAA International Air and Space Symposium and Exposition: The Next 100 Years*, AIAA Paper 2003-2659, 2003, <https://doi.org/10.2514/6.2003-2659>.
- [6] Vicroy, D., "X-48B Blended Wing Body Ground to Flight Correlation Update," Tech. Rept. HQ-STI-11-019, 2011.
- [7] Spearman, M. L., "Design Trends for Army/Air Force Airplanes in the United States," NASA TM-4179, 1990.
- [8] Larrimer, B. I., "Beyond Tube-and-Wing: The X-48 Blended Wing-Body and NASA's Quest to Reshape Future Transport Aircraft," NASA, 2020, pp. 87–97, 163–198.
- [9] Gray, A. L., Reist, T., and Zingg, D. W., "Further Exploration of Regional-Class Hybrid Wing-Body Aircraft Through Multifidelity Optimization," *AIAA Scitech 2021 Forum*, AIAA Paper 2021-0014, 2021, <https://doi.org/10.2514/6.2021-0014>.
- [10] Duvelleroy, M., and Benquet, L., "Airbus Reveals Its Blended Wing Aircraft Demonstrator," 2020, https://www.airbus.com/sites/g/files/jlcbita136/files/30215a68cdeef2eb6d3c4e4ab1b2b9c7_EN-MAVERIC-Airbus-reveals-its-blended-wing-aircraft-demonstrator.pdf.
- [11] Burley, C. L., Brooks, T. F., Hutcheson, F. V., Doty, M. J., Lopes, L. V., and Pope, D. S., "Noise Scaling and Community Noise Metrics for the Hybrid Wing Body Aircraft," *20th AIAA/CEAS Aeroacoustics Conference*, AIAA Paper 2014-2626, 2014, <https://doi.org/10.2514/6.2014-2626>.
- [12] Hileman, J., Spakovszky, Z., Drela, M., and Sargeant, M., "Airframe Design for "Silent Aircraft"," *45th AIAA Aerospace Sciences Meeting and Exhibit*, AIAA Paper 2007-0453, 2007, <https://doi.org/10.2514/6.2007-453>.
- [13] Dowling, A., and Hynes, T., "Towards a Silent Aircraft," *Aeronautical Journal*, Vol. 110, No. 1110, 2006, pp. 487–494, <https://doi.org/10.1017/S00019240000138X>.
- [14] Liebeck, R., Page, M., and Rawdon, B., "Blended-Wing-Body Subsonic Commercial Transport," *36th AIAA Aerospace Sciences Meeting and Exhibit*, AIAA Paper 1998-0438, 1998, <https://doi.org/10.2514/6.1998-438>.
- [15] Bolsunovsky, A., Buzoverya, N., Gurevich, B., Denisov, V., Dunaevsky, A., Shkadov, L., Sonin, O., Udzhuhu, A., and Zhurihin, J., "Flying Wing—Problems and Decisions," *Aircraft Design*, Vol. 4, No. 4, 2001, pp. 193–219, [https://doi.org/10.1016/S1369-8869\(01\)00005-2](https://doi.org/10.1016/S1369-8869(01)00005-2).
- [16] Clarke, J. P. B., Ho, N. T., Ren, E., Brown, J. A., Elmer, K. R., Tong, K. O., and Wat, J. K., "Continuous Descent Approach: Design and Flight Test for Louisville International Airport," *Journal of Aircraft*, Vol. 41, No. 5, 2004, pp. 1054–1066, <https://doi.org/10.2514/1.5572>.
- [17] Behere, A., Lim, D., Kirby, M., and Mavris, D., "Alternate Departure Procedures for Takeoff Noise Mitigation at Atlanta Hartsfield-Jackson International Airport," *AIAA Scitech 2019 Forum*, AIAA Paper 2019-2090, Jan. 2019, <https://doi.org/10.2514/6.2019-2090>.
- [18] Bertsch, L., Looye, G., Anton, E., and Schwanke, S., "Flyover Noise Measurements of a Spiraling Noise Abatement Approach Procedure," *Journal of Aircraft*, Vol. 48, No. 2, 2011, pp. 436–448, <https://doi.org/10.2514/1.C001005>.
- [19] Thomas, J., and Hansman, R. J., "Framework for Analyzing Aircraft Community Noise Impacts of Advanced Operational Flight Procedures," *Journal of Aircraft*, Vol. 54, No. 4, 2019, pp. 1407–1417, <https://doi.org/10.2514/1.C035100>.
- [20] "FAA's Proposal of a Stage 5 Aircraft Noise Standard," *LAX Community Noise Roundtable*, 2016, https://www.lawa.org/-/media/lawa-web/environment/lax-community-noise-roundtable/noise_management_presentations/noise_management_presentation/noisert_160309_stage-5-noise-standard.ashx.
- [21] Thomas, R. H., Burley, C. L., and Olson, E. D., "Hybrid Wing Body Aircraft System Noise Assessment with Propulsion Airframe Aeroacoustic Experiments," *International Journal of Aeroacoustics*, Vol. 11, Nos. 3–4, 2012, pp. 369–409, <https://doi.org/10.1260/1475-472X.11.3-4.369>.

- [22] Thomas, R. H., and Guo, Y., "Ground Noise Contour Prediction for a Nasa Hybrid Wing Body Subsonic Transport Aircraft," *23rd AIAA/CEAS Aeroacoustics Conference*, AIAA Paper 2017-3194, 2017. <https://doi.org/10.2514/6.2017-3194>
- [23] Kerrebrock, J. L., *Aircraft Engines and Gas Turbines*, 2nd ed., MIT Press, Cambridge, MA, 1996, Chap. 8.
- [24] Drela, M., "Transport Aircraft System OPTimization, Technical Description, Tech. Rept., Massachusetts Inst. of Technology, Cambridge, 2016, https://web.mit.edu/drela/Public/web/tasopt/TASOPT_doc.pdf.
- [25] Dedieu, J.-P., "Newton-Raphson Method," *Encyclopedia of Applied and Computational Mathematics*, Vol. 6, No. 7, 2015, pp. 1023–1028. https://doi.org/10.1007/978-3-540-70529-1_374
- [26] Thomas, J., and Hansman, R. J., "Community Noise Assessment of Hybrid-Electric Aircraft Using Windmilling Drag on Approach," *Journal of Aircraft*, Vol. 0, No. 0, 2021, pp. 1–11. <https://doi.org/10.2514/1.C036177>
- [27] Zorunski, W. E., "Aircraft Noise Prediction Program (ANOPP) Theoretical Manual, NASA TM-83199, Hampton, VA, 1982.
- [28] Kreja, E., and Stone, J., "Enhanced Fan Noise Modeling for Turbofan Engines," NASA CR 2014-218421, Glenn Research Center, Cleveland, OH, 2014.
- [29] Kontos, K. B., Kraft, R. E., and Gliebe, P. R., "Improved NASA-ANOPP Noise Prediction Computer Code for Advanced Subsonic Propulsion Systems. Volume 2: Fan Suppression Model Development," NASA CR 1996-202309, 1996.
- [30] Emmerring, J. J., Kazin, S. B., and Matta, R. K., "Core Engine Noise Control Program, Volume III, Supplement 1—Prediction Methods, Tech. Rept. FAA-RD-74-125, Vol. III-I, Washington, D.C., 1976.
- [31] Krejsa, E. A., and Valerino, M. F., "Interim Prediction Method for Turbine Noise," NASA TM X-73566, Cleveland, OH, 1976.
- [32] Stone, J., Groesbeck, D., and Zola, C., "An Improved Prediction Method for Noise Generated by Conventional Profile Coaxial Jets," NASA TM-82712, Lewis Research Center, Cleveland, OH, 1981.
- [33] Fink, M., "Airframe Noise Prediction Method," Tech. Rept. FAA-FRD-77-29, Washington, D.C., 1977.
- [34] Guo, Y., "An Improved Landing Gear Noise Prediction Scheme," NASA CR-NAS1-NNL04AA11B, The Boeing Company, Huntington Beach, CA, 2006.
- [35] Guo, Y., "Aircraft Slat Noise Modeling and Prediction," *16th AIAA/CEAS Aeroacoustics Conference*, AIAA Paper 2010-3837, 2010. <https://doi.org/10.2514/6.2010-3837>
- [36] Guo, Y., "Aircraft Flap Side Edge Noise Modeling and Prediction," *17th AIAA/CEAS Aeroacoustics Conference (32nd AIAA Aeroacoustics Conference)*, AIAA Paper 2011-2731, 2011. <https://doi.org/10.2514/6.2011-2731>
- [37] Hutcheson, F., Brooks, T., and Humphreys, W., "Noise Radiation from a Continuous Mold-Line Link Flap Configuration," *14th AIAA/CEAS Aeroacoustics Conference*, AIAA Paper 2008-2966, 2008. <https://doi.org/10.2514/6.2008-2966>
- [38] Maekawa, Z., "Noise Reduction by Screens," *Applied Acoustics*, Vol. 1, No. 3, 1968, pp. 157–173. [https://doi.org/10.1016/0003-682X\(68\)90020-0](https://doi.org/10.1016/0003-682X(68)90020-0)
- [39] Bradley, M. K., and Dronney, C. K., "Subsonic Ultra Green Aircraft Research: Phase 2," NASA CR-2015-218704/VOL2, 2015.
- [40] Naik, A. M., Listgarten, N., Recine, C., Kinney, D., Binzley, R., Jain, A., and James, K. D., "System Noise Analysis Methodology and Results for EPFD and SFD Vehicles," *AIAA AVIATION FORUM AND ASCEND 2024*, AIAA Paper 2024-3915, 2024. <https://doi.org/10.2514/6.2024-3915>
- [41] SAE International, "Standard Values of Atmospheric Absorption as a Function of Temperature and Humidity," *SAE ARP866A*, 1975.
- [42] Chien, C., and Soroka, W., "Sound Propagation Along an Impedance Plane," *Journal of Sound and Vibration*, Vol. 43, No. 1, 1975, pp. 9–20. [https://doi.org/10.1016/0022-460X\(75\)90200-X](https://doi.org/10.1016/0022-460X(75)90200-X)
- [43] SAE International, "Method for Predicting Lateral Attenuation of Airplane Noise," *SAE AIR 5662*, 2006.
- [44] . "Noise Standards: Aircraft Type and Airworthiness Certification," Code of Federal Regulations, Federal Aviation Administration, Department of Transportation, FAR Part 36, 2018, <https://www.ecfr.gov/current/title-14/part-36>.
- [45] . "Annex 16 to the Convention on International Civil Aviation. Environmental Protection," ICAO Standard and Recommended Practice, 8th ed., Vol. 1, ICAO, Montreal, QC, Canada, 2017, <https://store.icao.int/en/annex-16-environmental-protection-volume-i-aircraft-noise>.
- [46] Raymer, D. P., Wilson, J., Perkins, H. D., Rizzi, A., Zhang, M., and Puentes, A. R., "Advanced Technology Subsonic Transport Study, N+3 Technologies and Design Concepts," NASA TM-2011-217130, 2011.
- [47] Commission, E., "Flightpath 2050 Europe's Vision for Aviation," SAE Committee A-21, European Commission, 2011. <https://doi.org/10.2777/50266>
- [48] Sun, J., Hoekstra, J. M., and Ellerbroek, J., "Aircraft Drag Polar Estimation Based on a Stochastic Hierarchical Model," 2018, <https://api.semanticscholar.org/CorpusID:126512803>.
- [49] Company, T. B., "737-600/700-800/900 Operations Manual," 1997, <https://toulouse747.com/wp-content/uploads/2018/12/Boeing-B737-700-800-900-Operations-Manual.pdf> [retrieved 22 Nov. 2023].
- [50] Kontos, K. B., Janardan, B. A., and Gliebe, P. R., "Improved NASA-ANOPP Noise Prediction Computer Code for Advanced Subsonic Propulsion Systems Volume 1" ANOPP Evaluation and Fan Noise Model Improvement," NASA CR-195480, GE Aircraft Engines, Cleveland, OH, 1996.
- [51] U.S. Government Publishing Office, "14 CFR Part 25—Airworthiness Standards: Transport Category Airplanes — US Law — LII / Legal Information Institute," 2017, <https://www.law.cornell.edu/cfr/text/14/part-25>.
- [52] Clark, I. A., Thomas, R. H., and Guo, Y., "Aircraft System Noise of the NASA D8 Subsonic Transport Concept," *Journal of Aircraft*, Vol. 58, No. 5, 2021, pp. 1106–1120. <https://doi.org/10.2514/1.C036259>
- [53] Yu, A., and Hansman, R. J., "Approach for Representing the Aircraft Noise Impacts of Concentrated Flight Tracks," *AIAA Aviation 2019 Forum*, AIAA Paper 2019-3186, 2019. <https://doi.org/10.2514/6.2019-3186>

M. Snellen
Associate Editor